

# Simulation of Grasping Deformable Objects with a Virtual Human Hand

Tong Cui, Jing Xiao, Senior Member, IEEE, Aiguo Song

**Abstract**—This paper addresses a largely open problem in haptic simulation and rendering: contact force and deformation modeling for haptic simulation of grasping a deformable object with a realistic virtual human hand, especially in power grasps. The virtual hand model consists of meshes of realistic shapes for the finger links and palm of a hand. We tackle the problem by adopting the non-linear contact force model and the beam-skeleton model for global shape deformation introduced in [5]. The results verify the efficiency of contact force and deformation modeling for both power grasp and precision grasp of deformable objects with reasonable realism.

## I. INTRODUCTION

Modeling deformable objects under contact or manipulation have been studied for many applications, such as virtual training in surgery operations, haptics, planning of grasping in robotics, tele-robotic operations, etc. In particular, several algorithms employ continuous elasticity theory to model the interaction between a human hand and deformable objects. In order to show how surface deformations may be taken into account in the modeling of static surface forces, Barthel presented a simple model [1] to describe qualitatively the behavior of elastic surfaces submitted to an oscillatory force field. Kuroda *et al.* [2] introduced a training environment for deformable exclusion with a basic study of multi-finger haptic interaction. Previous research is mainly focused on fingertip grasps, where contacts happen on isolated points or regions and cause only local deformation on the grasped deformable object. In addition, most hand models in existing work are made of simple rigid parts such as sticks and spheres, which makes the hand model rough and unrealistic compared with a true human hand. This is for the sake of increasing computational efficiency to achieve real-time interaction.

In reality, however, a human hand is rather complex in shape and with a large number of degrees of freedom (DOF) [3, 4]. Modeling full-hand real-time interaction with

deformable objects is all the more challenging, and is largely an open problem. On the other hand, being able to simulate full-hand haptic interaction with deformable objects in real time is potentially useful for robotic applications involving “learning-by-demonstration”, especially in tele-operations.

Recently, Luo and Xiao introduced a novel and efficient model to force and deformation modeling between a rigid object and an elastic object in interactive environments [5]. The approach is characterized by modeling nonlinear contact forces based on the Duffing equations and using a “beam-skeleton” model based on the beam bending theory to simulate global shape deformation.

In this paper, we introduce a realistic virtual hand model with all the DOFs of a human hand and with meshes of realistic shapes to model the links. We then extend the approach of [5] to modeling the interaction between such a realistic human hand and an elastic object, including various ways of grasping, especially the enveloping power grasps, which cause multiple contact regions and large, global deformation of the object grasped. Our work provides a good solution to the problem of modeling full-hand interaction with deformable objects, balancing real-time efficiency and physical realism.

The paper is organized as follows: In Section II, we introduce our virtual hand model and the related contact geometry during grasping. In Section III, we review related work, and in Section IV, we describe simulation of grasping deformable objects. In Section V, we discuss implementation and experimental results, and we conclude the paper in Section VI.

## II. HAND AND GRASP MODELING

We design a dexterous hand model by dividing the whole hand into two sections: a dexterous work set (5 fingers) that allows the hand to maintain a stable grasp while manipulating an object, and a supporting palm. The dexterous work set has a total of 21 DOF: the thumb has 5 DOF, and each of the other fingers has 4 DOF. Each finger link (including the palm) is a rigid body of realistic shape represented by a triangle mesh. The dimensions of each phalanx of fingers have been measured [6]. The entire hand mesh model consists of 5024 triangles with 2015 vertices.

To model grasping with the hand model, we divide each finger into three parts, which are the three burls, as shown in Fig. 1. These parts correspond to three potential contact regions for each finger. Thus, there are a total of fifteen parts that can be in contact with an object during a power grasp,

Manuscript received February 22, 2008. This work was supported in part by the U.S. National Science Foundation under Grant IIS-0328782 and the National Basic Research Development Program of China (973Program) (No. 2002CB312102), the National Natural Science Foundation of China (No. 60475034, 60643007), the National High Technology Research and Development Program of China (863Program) (No. 2006AA04Z246) and 2007 Graduate Science and Technology Innovation Plan of Jiangsu Province.

Tong Cui and Jing Xiao are with the IMI Lab, Department of Computer Science, University of North Carolina – Charlotte, Charlotte, NC 28223, USA. E-mails: tcui@uncc.edu, xiao@uncc.edu.

Tong Cui is a visiting scholar at the above institution. He and Aiguo Song are also with College of Instrument Science and Engineering, Southeast University, Nanjing 210096, P.R.China.

exert forces to the object, and if the object is elastic, cause the object to deform. Note that we do not consider the palm to cause deformation of the object, but rather it only supports the object to make the grasp stable, i.e., the force it exerts to the object balances the other forces exerted to the object.

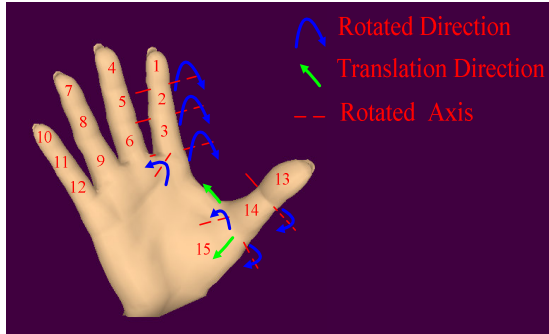


Fig. 1 Hand model

### III. REVIEW OF RELATED WORK ON CONTACT AND DEFORMABLE MODELING

This section briefly reviews the approach for contact and deformation modeling between a rigid body and an elastic object introduced earlier [5], which we will extend here to model full-hand grasping of deformable objects.

#### A. Basic Assumptions

Contacts are considered between a rigid object and an elastic object in a virtual environment. Both objects have mesh models. The elastic object is convex with smooth surface patches when undeformed, and there is a parametric model of the originally undeformed surface. The interaction between the rigid object and the elastic object is sufficiently slow so that contact forces are caused by quasi-static collisions, and shape deformation of the elastic object only occurs at stable equilibrium configurations, where the elastic energy is minimized. Each contact region is relatively small comparing to the size of the elastic object. There can be multiple contact regions between the rigid object and the elastic object at the same time, but multiple contact regions are assumed to be formed one by one. This last assumption is reasonable because the chance that two contacts occur at exactly the same time is rather small, and “simultaneous” contacts can be modeled as contacts that occur at instants very close to one another.

#### B. Contact Force and Shape Deformation Modeling

The approach reported in [5] can handle contact and deformation modeling for interactive environments, where both visual feedback and haptic feedback are needed.

A nonlinear model is used to simulate contact forces exerted to the held rigid object from the elastic object under point contact, and the model is extended to general non-point contacts.

Both global deformation of the entire elastic object and local deformation within neighborhoods of contact regions

are modeled. In order to handle the global shape change due to deformation, a novel “beam-skeleton model” with respect to a contact region is introduced to compute the distribution of stresses and strains of a deformed elastic object at certain “anchor points” defined on the original, undeformed surface of the object.

An anchor point is a natural vertex, a curvature discontinuous point, a discontinuous point of the first derivative of curvature, a point with local minimum or maximum curvature, or an inflection point with zero curvature [7]. For a circular edge (such as on an object of revolution), four points evenly distributed on the circle are chosen as anchor points based on the Four Vertex Theorem in differential geometry [8]. For a sphere, there are six evenly distributed anchor points. Fig. 4 shows the anchor points of a cylinder and a sphere.

At each anchor point, the computation of stress and strain is based on applying the Bernoulli–Euler bending beam theory. Next, fast computation of global shape change is realized through an interpolation method that achieves minimization of the elastic energy.

Both contact force and shape deformation effects of multiple contact regions are modeled by building beam-skeletons and computing shape deformation based on the temporal order of contact regions (since contact regions are assumed to be formed one by one).

### IV. SIMULATION OF GRASPING DEFORMABLE OBJECTS

Grasping an object with a human hand can involve some parts of fingers, some fingers, or all fingers contacting the object. With an elastic object, any kind of grasp will cause deformation of the object shape. A power grasp, in particular, is formed by enveloping the object to be grasped, which can cause severe deformation of the elastic object. With the hand model introduced in section II, a grasp can be generally viewed as having some parts or all parts of the fingers (out of the 15 parts shown in Fig. 1) contact the elastic object.

When a contact occurs between a part of the hand and the elastic object, the force exerted from the hand to the elastic object can be computed from the deformation displacement of the contact region of the elastic object based on the nonlinear Duffing equation [5].

We next focus on modeling the shape deformation of the elastic object due to the forces exerted to the object from the hand in a grasp. Our approach can be divided into two steps: (1) global deformation computation based on the beam-skeleton model, (2) modification based on merging contact regions and on considering local nonlinear deformation.

#### A. Global Deformation

A beam-skeleton [5] can be established for each contact region, corresponding to the contact between a part of the hand (out of the 15 parts shown in Fig.1) and the elastic object. The beam skeleton is formed by connecting the force-equivalent point of the contact region to each anchor

point of the elastic object by a beam (see Fig. 2). The force exerted from the hand to the elastic object at the contact region is distributed to the beams, based on the thickness and length of each beam [5]. Each force applied to a beam causes a strain and a stress at the other end of the beam, i.e., an anchor point, which can be computed based on the Bernoulli-Euler bending beam theory. From the strain and stress, the corresponding deformation displacement of an anchor point can be computed.

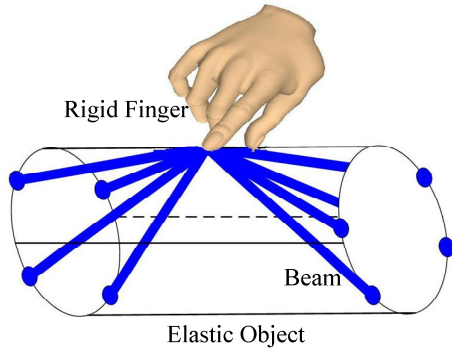


Fig. 2 Beam skeleton (in blue solid lines) on an elastic cylinder object corresponding to one contact

Since multiple contact regions occur during a grasp one by one in a temporal order (see section II), their combined effects on an anchor point can be computed accordingly in the same order. As a beam skeleton is established for each contact region one by one, for any anchor point of the elastic object, we can see multiple beams from multiple contact regions occur one by one, and each beam is connected to the position of the anchor point as the result of accumulated deformations from beams established previously. Figure 3 shows an example, where Beam 2 from a contact region 2 is established after Beam 1 (from a contact region 1) and connects the position of the anchor point after its deformation due to Beam 1. Subsequently, Beam 3 from a contact region 3 is established after Beam 2, connecting to the position of the anchor point resulted from the combined deformation effects due to Beam 1 and Beam 2.

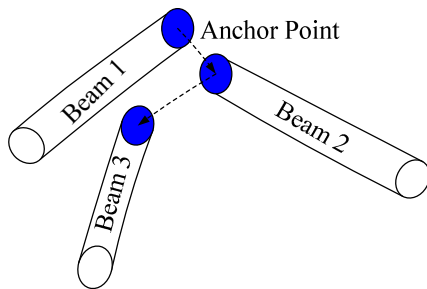


Fig.3 The deformation displacement of an anchor point due to multiple contact regions.

The global shape deformation of the elastic object can be obtained by interpolating the deformation displacements of

the anchor points over the entire surface of the elastic object via an interpolation method based on RBF [9]. Note that the shape of a contact region on the elastic object is the same as the shape of the contacting part on the hand. As contact regions happen one by one in a grasping process, each intermediate shape deformation of the elastic object corresponding to the already happened contacts can be obtained before a final grasp is achieved. The deformed shape of the elastic object under a stable grasp is the result of all contact regions in the grasp. In the case of a power grasp, there are 15 contact regions at the 15 parts of the hand. Note that the palm can be considered flat and much larger than the other contact regions and thus does not cause shape deformation other than flattening the region of the elastic object it contacts.

### B. Merged Contact Regions and Local Deformation Adjustment

If two contact regions between two adjacent parts of a finger and the elastic object are very close neighbors, they may be merged into one contact region under heavy deformation. After the merge, the portion of the elastic object inside the merged contact region but is not part of the original contact regions takes the shape of the finger region between the two parts that form the two original contact regions (i.e., the joint region between two finger links). More than two contact regions can be merged in this fashion to a larger contact region. After the merge, there can be just a few large and fairly separated contact regions.

Within a small neighborhood of each separate contact region, the deformation at each point is actually a logarithmic function with respect to the distance to the contact region [10]. Thus, the global shape deformation (as the result of linear interpolation of deformations at anchor points) is modified to reflect this property.

### C. Contact Forces in Grasping

In the process of grasping, multiple contacts are formed one by one between the hand and the elastic object. The total force  $F_i$  exerted from the hand to the elastic object (and vice versa) at a contact region  $i$  in a stable grasp can be obtained as:

$$F_i = F_{s_i} + \sum_j F_{s_j}$$

where the first term is the force caused by the deformation displacement due to the  $i$ -th contact (on top of the deformed shape due to contacts occurred before  $i$ ), which can be computed from the Duffing equation [5], and the second term is the sum of force effects from the contact regions formed after the contact region  $i$ . The force effect of each contact region  $j$  occurred after the  $i$ -th contact is computed by interpolation of the stresses computed from the beam skeleton of  $j$  at related anchor points.

The total contact force is the sum  $\sum F_i$  of forces from all contact regions.

## V. IMPLEMENTATION AND EXPERIMENTAL RESULTS

Our implementation is done in a virtual environment on a PC with dual Intel Xeon 2.4 GHz Processors and 1 GB system RAM. The virtual hand model can be either controlled by keys on the computer keyboard or via a haptic device for real-time interaction with a virtual elastic object made of rubber. The bottom center of the elastic object is fixed, where a world coordinate system is set.

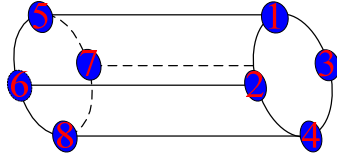
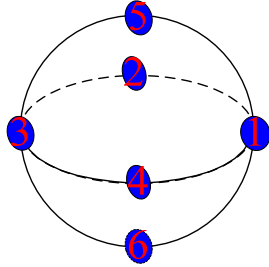


Fig. 4 (a) Anchor points of a cylinder



(b) Anchor points of a sphere

TABLE I  
HAND MODEL PARAMETERS

Finger parts	Width (mm)	Length (mm)	#Contact Meshes	Local Neighborhood Radius (mm)	
<i>First finger</i>	1	12	25.1	18	10
	2	12	21.5	18	10
	3	12	26.9	18	10
<i>Middle finger</i>	4	15	27.2	21	12
	5	16	24.3	26	13
	6	17	30.3	26	14
<i>Ring finger</i>	7	12	25.2	12	10
	8	12	20.9	18	10
	9	12	27.2	30	10
<i>Little finger</i>	10	8	18.9	14	7
	11	9	15.6	26	7
	12	10	16.8	32	8
	13	15	26.9	28	18
<i>Thumb</i>	14	14	33.5	42	13
	15	14	38.9	28	10

TABLE II  
PARAMETERS OF ELASTIC OBJECT USED IN EXPERIMENTS

Parameter	Cylinder	Sphere
$M(kg)$	1.43	1.60
$\beta_0^2 \varepsilon$	0.4	0.4
$\omega_0$	0.2	0.2
$I(kg/cm^2)$	102	104
$E(N/m^2)$	$3 \times 10^6$	$3 \times 10^6$
$\nu$	1.0	1.0

We have tested our program by making our virtual hand to grasp virtual rubber objects of different shapes in different kinds of grasps. Figure 4 (a) shows a cylindrical object and its 8 anchor points, and Fig. 4 (b) shows a sphere and its 6 anchor points (see section III.B for determination of anchor points).

Table I and Table II list the parameters of the hand model and that of elastic objects of different shapes and sizes used in experiments. Table I shows the length and width of each finger part. “Contact meshes” of each part  $i$  of a finger define the area most likely in contact if part  $i$  is contacting the deformable object. The local neighborhood radius for each part  $i$  define a neighborhood including the contact region, such that each non-contact point of the elastic object in the neighborhood is subject to local deformation adjustment. And the weight of each finger part is 0.1 kg.

Table II shows the parameters of the two elastic objects in experiments.  $\omega_0$ ,  $\beta_0^2 \varepsilon$  are the parameters of linear and nonlinear restoring terms respectively in Duffing equations.  $M$  is the weight of the elastic object,  $E$  is the Young’s modulus,  $I$  is the moment of inertia, and  $\nu$  is Poisson’s ratio [5].

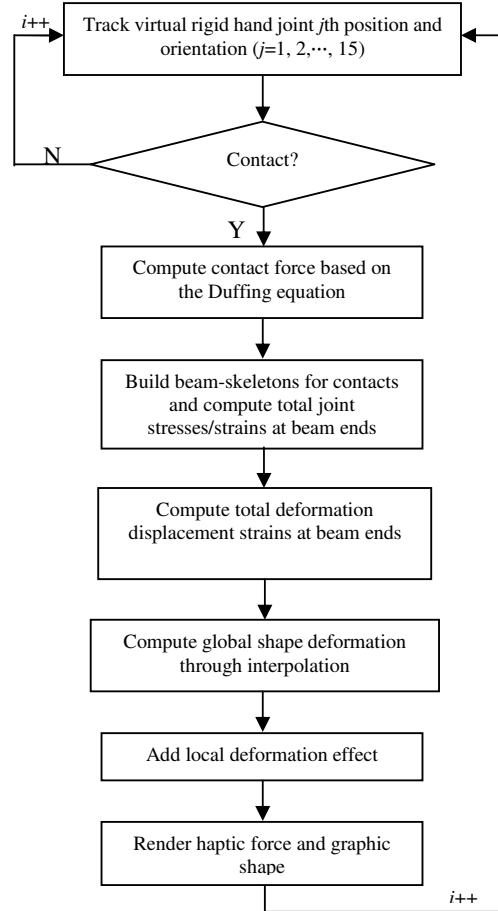


Fig. 5 Program flowchart

Fig. 5 shows the flow chart of our program, where each iteration indicates one time-step “update” of contact force and resulting shape deformation.

To grasp an object, either a preshape of the virtual hand is determined automatically based on the shape and pose of the object [11], or the preshape of the virtual hand can be decided interactively by a human user using an input device. In our experiments, since we do not have a data glove, we use different keys on a keyboard to interactively control different fingers or different joints on a finger to achieve a grasp of the virtual deformable object by the virtual hand in real-time. In the process, our algorithm for real-time simulation of contact force and shape deformation provides real-time rendering of the changing shape of the elastic object and the time series of the contact forces.

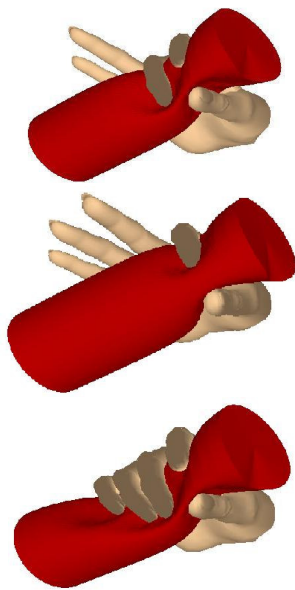


Fig. 6 Different grasps of the cylindrical object and the resulted shape deformation

Figure 6 shows three different kinds of grasps on the cylindrical rubber object, using two fingers, three fingers, and five fingers (power grasp). The deformed shapes of the cylindrical object are the results of shape deformation modeled by our program.

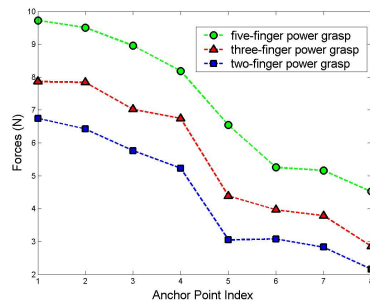


Fig. 7 Comparing stresses at different anchor points of the cylindrical elastic object under different grasps

Figure 7 shows the result of comparing stresses at each of the 8 anchor points of the cylindrical objects for the three different grasps shown in Figure 6. The stress amount shown was measured when a stable grasp was achieved. In all three cases, the time for each finger to achieve its final grasping state is the same to ensure fair comparison. We can see that among the three different grasps, the five-finger power grasp (where all 15 parts of the fingers are contacting the object) create the most amount of stresses at the anchor points and the most severe deformation of the object. For each grasp, the anchor points closer to the contact regions are under greater stresses, which is reasonable. There is a big drop of stress level between anchor point 4 and anchor point 5 in every case, because of the big increase of distance to the contact regions from anchor point 5, but this drop of stress is less steep for the five-finger power grasp because the contact regions are larger and closer to all the anchor points. Also note that as the hand approached the cylindrical object from the side defined by anchor points 1, 2, 5 and 6, the stresses at the anchor points happen to decrease as the anchor index increases.

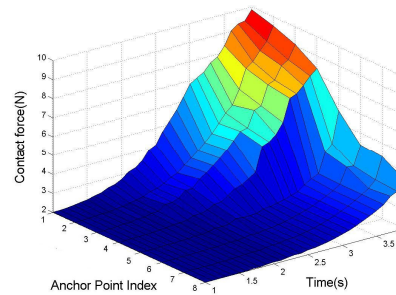


Fig. 8 Stresses at anchor points as a function of time during a five-finger power grasp.

Figure 8 depicts of the stress at each anchor point of the cylindrical object as a function of time during the five-finger power grasp process until a stable grasp is achieved. The stress at each anchor point starts from zero and increases to the maximum amount when a stable grasp is achieved.

Fig. 9 shows another example with three different kinds of grasps on a rubber sphere, which has six anchor points.

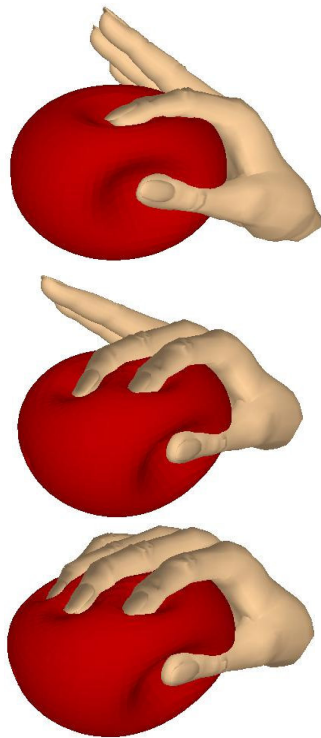


Fig. 9 Different grasps of the spheric object and the resulted shape deformation

TABLE III  
RUNNING TIME PER UPDATE FOR THE FIVE-FINGER POWER GRASPS OF DIFFERENT OBJECTS

Parameter	Cylinder	Sphere
<i>Mesh</i>	3024	3480
<i>Vertices</i>	1514	1742
<i>Avg. collision check cost per update (ms)</i>	5.520	5.815
<i>Avg. time for contact force and shape simulation per update (ms)</i>	1.80	2.62
<i>Avg. drawing time per update(ms)</i>	1.25	1.26
<i>Total #updates</i>	160	120

Table III shows the running time of our algorithm per update (or the time step running cost). The total time per update includes (a) the time for contact detection, (b) the time for contact force and shape deformation modeling, and (c) the time for updating the graphic display. Obviously, among the three update time costs, the focus of this paper—the modeling of contact force and shape deformation in grasping takes the least time, which is actually good enough for effective haptic simulation. Note that the virtual hand model is very complex, and its mesh has a very large number of triangles to be realistic, and the deformable objects in these examples, though look simple, also have meshes of large number of triangles. Thus, the small updating time of our

contact force and deformation modeling approach shows its efficiency and effectiveness in modeling realistically complex multi-contact situation, as characterized by power grasps of deformable objects.

Note that we did not use the most efficient methods or hardware for contact detection. With more efficient methods, the update costs for collision detection can be significantly improved.

## CONCLUSION

We proposed a fairly realistic human hand model and modeled the contact force and shape deformation during the process of grasping an elastic object by such a virtual hand. There are up to 15 contact regions between the virtual hand fingers and the elastic object during a grasp. In the case of a power grasp, all 15 contact regions occur. Our model of contact force and shape deformation for grasping balances well the need for real-time efficiency and for realism in an interactive environment. We are currently investigating how to further increase efficiency and extending this work to simulate grasping non-convex deformable objects or deformable objects with holes.

## REFERENCES

- [1] E. Barthel, "Surface Deformation, Spring Stiffness and the Measurement of Solvation Forces," *thin Solid Films*, 330(1): 27-33, September 1998.
- [2] K. Tomohiro, M. Yasushi, O. Osamu, "Construction of Training Environment for Surgical Exclusion with a Basic Study of Multi-finger Haptic Interaction," *Euro Haptics Conference, 2007 and Symposium on Haptic Interfaces for Virtual Environment and Teleoperator Systems*, March 2007, pp. 525-530.
- [3] T. Heap, D. Hogg, "Towards 3D hand tracking using a deformable model," *the Second International Conference on Automatic Face and Gesture Recogniti*, pp.140-145, 1996.
- [4] G. Stellin, G. Cappiello, S. Roccella, M.C. Carrozza, P. Dario, G. Metta, G. Sandini, F. Becchi, "Preliminary Design of an Anthropomorphic Dexterous Hand for a 2-Years-Old Humanoid: towards Cognition," *The First IEEE/RAS-EMBS International Conference on Biomedical Robotics and Biomechatronics*, pp.290-295,2000.
- [5] Q. Luo, J. Xiao, "Contact and Deformation Modeling for Interactive Environments," *IEEE Transactions on Robotics*, 23(3): 416-430, June 2007.
- [6] F.Lotti, G.Vassura, "A novel approach to mechanical design of articulated fingers for robotic hands," *IEEE International Conference on Intelligent Robots and Systems*, Oct. 2002, pp.1687 -1692.
- [7] S. Tabachnikov, "The four-vertex theorem revisited—Two variations on the old theme," *Amer. Math. Monthly*, 102:912-916, 1995.
- [8] T. Belytschko, W. Liu, and B. Moran, *Nonlinear Finite Elements for Continua and Structures*, New York: Wiley, 2000.
- [9] M.J.D. Powell, "The theory of radial basis function approximation," *Algorithms and Radial Functions*, vol. II, Oxford University Press, Oxford, 1990, pp. 105-210.
- [10] Q. Luo and J. Xiao, "Geometric Properties of Contacts Involving a Deformable Object," *IEEE Symposium on Haptic Interfaces for Virtual Environment and Teleoperator Systems*, Washington D.C., March 25--26, 2006, pp. 533-538.
- [11] Y. Li, N.S. Pollard, "A Shape Matching Algorithm for Synthesizing Humanlike Enveloping Grasps," *5th IEEE-RAS International Conference on Humanoid Robots*, Dec. 2005, pp. 442- 449.